ASSEMBLED CORNER-CUBE RETROREFLECTOR QUADRUPLET

Lixia Zhou, Kristofer S. J. Pister and Joseph M. Kahn

Department of Electrical Engineering and Computer Sciences

University of California, Berkeley, CA 94720 USA, {lzhou, pister, jmk}@eecs.berkeley.edu

ABSTRACT

A MEMS corner-cube retroreflector (CCR) is presented. It is used as the free-space optical communication transmitter in the Smart Dust project. The optical and electrical properties are greatly improved as compared to CCRs fabricated previously in the MUMPS process[1, 2]. Improvements include a tenfold improvement in mirror curvature, a threefold reduction of mirror misalignment, a fivefold reduction of drive voltage, a tenfold increase in resonant frequency, and an improved scalability due to the quadruplet design.

INTRODUCTION

A corner-cube retroreflector (CCR) consists of three mutually orthogonal mirrors that form a concave corner. MEMS CCRs have been designed to work as passive transmitters in a free-space optical communication system for the Smart Dust project. High-performance CCRs require flat, accurately aligned mirrors and, as three-dimensional structures, pose challenges to MEMS fabrication technology. Low actuation voltage and high-speed operation are important factors in the Smart Dust application.

Surface micromachining processes inherently produce two-dimensional thin-film structures. Three-dimensional structures may be achieved by rotating plates out of plane on hinges. Previous CCR fabricated in the MUMPS process were assembled in this way[1, 2]. These CCRs had poor-quality mirror surfaces, and the hinges were not able to provide sufficiently accurate mirror alignment.

SOI technology offers significant benefits for CCR fabrication. Mirror flatness is no longer an issue. Bulk micromachining makes possible high actuation force and low actuation voltage. A fully
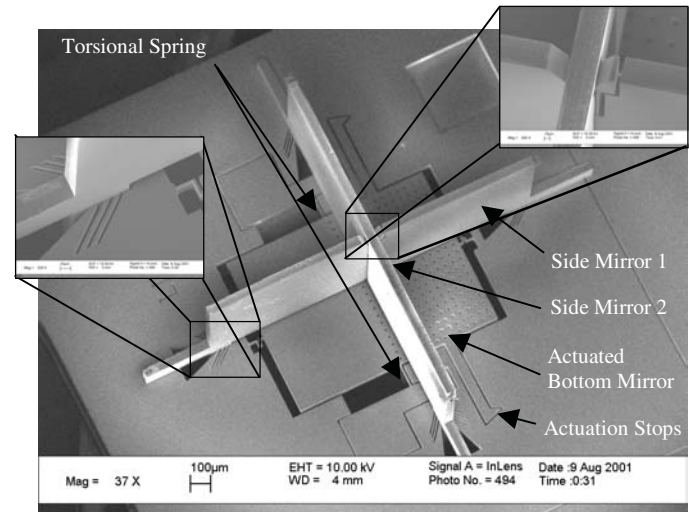

Figure 1: A quad-CCR with single bottom-plate actuation. Note the spring-locks on top and bottom of the 50um thick assembled side mirrors, and the limit stops which land on electrically isolated substrate islands.

locked-in structure is able to maintain orthogonal alignment of the side mirrors.

DESIGN AND FABRICATION

The SEM picture in figure 1 shows a fabricated and assembled CCR. Two side mirrors sit on the chip, while the bottom mirror is designed to be torsionally actuated so that it can modulate the outgoing light direction.

We have chosen to fabricate CCRs in a SOI process to obtain flat and smooth mirror surfaces. In the Smart Dust project, a CCR is illuminated by an interrogator, and an angle displacement of one CCR mirror switches the light reflected from the CCR between the '0' and '1' states. This angle displacement needs to be only several mrad for communication over kilometer distances. The device layer and substrate layer of the SOI wafer can form the opposing electrodes of a gap-closing actuator, while the narrow gap formed between them provides for a device plate deflection of several mrad and enables high actuation force at

low drive voltage. The actuated device plate is suspended by two torsional springs. The extended device layer beam and an electrically isolated substrate island act as the mechanical stop to prevent shorting between the plates after pull-in. The triangular shaped stop creates a contact point at the pull-in position so that the stiction is minimized to ensure release of the actuated plate. There is another advantage of designing the gap-close stop in this way. The extended beam allows us to decouple the sizing of the actuated mirror and of the actuator. We size the actuated mirror to satisfy optical requirements for the required communication distance, while we size the actuator to achieve low drive voltage and sufficient angular deflection. Two side mirrors are placed on top of the substrate, anchored by inserting small feet into spring-loaded slots in the substrate. Springs on each of the side mirrors lock the side mirrors together, maintaining accurate alignment. In this way, we can naturally fabricate four CCRs that share a common actuated bottom mirror, although the performance of those four CCRs may differ due to the asymmetrical positioning of side mirrors and the presence of etching holes. We place the side mirrors in such an asymmetrical way so that the optical performance of one CCR out of four is optimized while minimizing the overall size of the device.

The process flow is shown in Figure 2. The fabrication starts with a double-side-polished SOI wafer with a 50 μm device layer thickness and a 2 μm buried oxide layer thickness. First approximately a 1 μm thick thermal oxide was grown on both sides of wafer at 1100 °C. We patterned the front-side oxide with the device layer
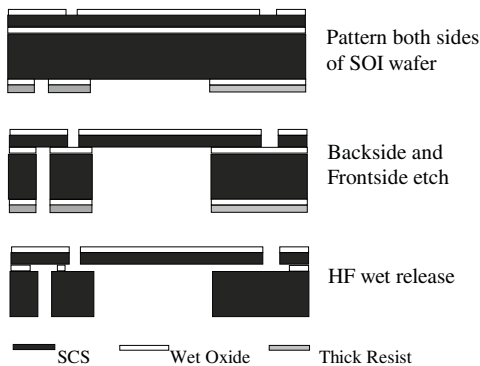

Figure 2: Bottom mirror fabrication process. The backside etch allows electrically isolated islands in the substrate.

mask. The main structure is on this layer, including the bottom mirror, two torsional spring beams suspending the bottom mirror, gap-closing actuation stops and positioning slots for anchoring side mirrors. Then we flipped the wafer over, deposited thick resist and patterned the back-side oxide with the substrate layer mask. The substrate layer functions as the other node of the actuator and provides structural support for the CCR structure. We begin the STS etch with backside first. After etching through the substrate, we etch the buried oxide away, releasing the possible stress which may otherwise present during the frontside etch. Then we etched the frontside trenches using STS. After etching, the whole chip is dipped into HF for about 10 min, to remove the sacrificial oxide film between the bottom mirror and substrate. There is no need to use the critical point dryer after releasing because the tie-downs between the mirror and the rest of chips are holding the mirror in place,
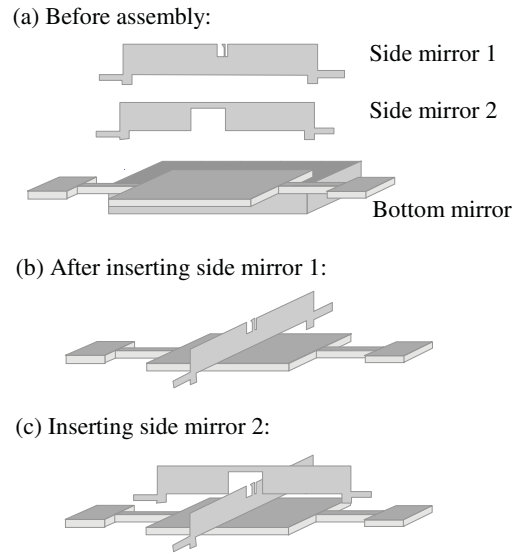

Figure 3: Assembly sequence.

preventing it from being attracted to the substrate.

Side mirrors can be generated in the same process or by another standard single-mask process. We patterned the device layer of SOI wafer with the shape of side mirrors, followed by a long time HF release. When both bottom mirror and side mirrors are ready, we mount the side mirrors onto the bottom mirror manually to form a fully functional CCR. Figure 3 shows the scheme of assembly. First we pick up side mirror 1, using a pair of fine-tip tweezers. We insert it into the slot around the
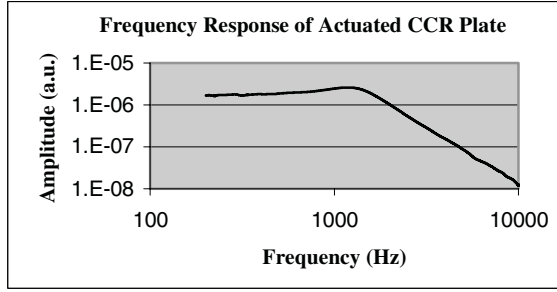
Frequency Response of Actuated CCR Plate

Figure 4: Frequency response of actuated CCR plate.
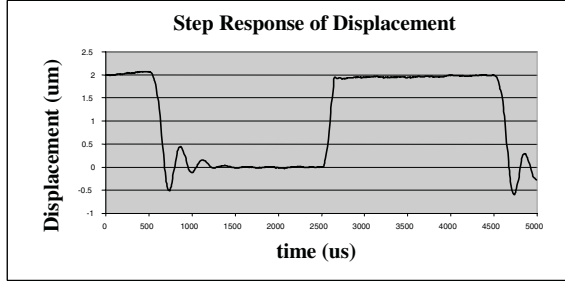
Step Response of Displacement

Figure 5: Step response. Compare the ringing of the plate on release at 1000us to the abrupt pull-in at 2500 us.

bottom mirror. Then we pick up side mirror 2 and insert into the perpendicular slot. When both mirrors are pushed to the end of slot, the spring-loaded design ensures that the side mirrors are in the correct place. The assembly is done under a stereo microscope. After assembly, we use a probe station to finely tune the position of side mirrors and use UV-curable epoxy to secure the side mirrors to the chip.

As silicon reflects around 30 percent of visible light, a gold deposition can greatly improve the optical performance of CCR. We evaporate a 50 nm-thick layer of gold after assembly.

CHARACTERIZATION

A gap-closing actuator, suspended by torsional beams, has pull-in position and pull-in voltage of

$$\theta_{pull-in} = 0.4404 \cdot \frac{g}{W_m}$$

$$V_{pull-in} = \left(\frac{9.685 \cdot K_\theta \cdot \theta_{pull-in}^3}{\varepsilon_0 \cdot L_m} \right)^{1/2}$$

where g is the gap distance of the actuator, i.e., the thickness of insulated oxide layer in SOI wafer.

W_m and L_m are the width and length of the actuator plate. K_θ is the torsional spring constant. Notice that θ_{full}, the full angular travel of the actuator, is g/W_m, which is several mrad for a gap width of 2 μm and a plate size of 500 μm, and meets the requirement for long-distance communication.

The resonant frequency of actuated plate is given by

$$f = \frac{1}{2\pi} \left(\frac{K_\theta}{I_m} \right)^{1/2}$$

where I_m is the moment of inertia of the actuated plate.

Experiment demonstrate a DC pull-in voltage as low as 5 V and a pull-in angle of approximately $0.44\theta_{full}$, in good agreement with theoretical predictions. Figure 4 shows the frequency response of one device, measured using a POLYTEC laser Doppler vibrometer. The resonant frequency occurs at 1.3 kHz while the 3-dB cut-off frequency is around 2.1 kHz. A higher resonant frequency is achievable by decreasing the thickness of device layer of SOI wafer.

The step response of CCR is shown in figure 5. Since the CCR exhibits a relatively high Q factor, there is overshoot when actuated plate is free from voltage actuation. The bottom plate vibrates about its unactuated position before settling down. The settling time is around 1 ms, giving a maximum data transfer rate of about 1 kps.

The optical experimental setup shown in Fig. 6 was used to measure the far-field diffraction pattern of the assembled CCR. Figure 7a shows the far-field pattern of the light reflected by the CCR on the "1" state, with illumination along the CCR body diagonal direction, while figure 7b shows the theoretical simulation for the perfect CCR of the same size[3]. They exhibit similar "star" patterns, corresponding to an effective reflecting area[3] of a six-sided polygon. The angular period between different diffraction orders shows the similiarity, with the experiment result of 1.2 mrad and theoretical result of 1 mrad in one direction.

The differential scattering corss section (DSCS) is defined to measure the optical performance of CCR, and is given by[1]
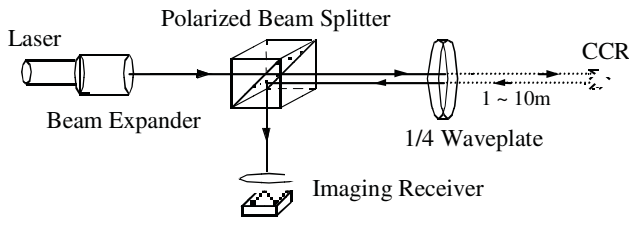
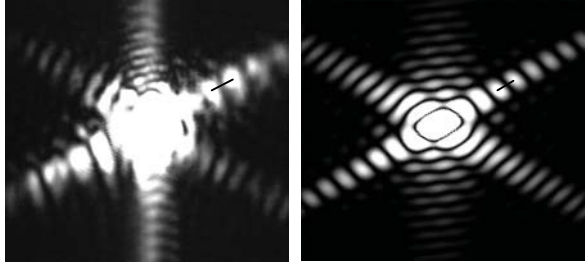Figure 6: Optical setup for uplink communication

Figure 7: Far-field patterns of light reflected from CCR. Left: experimental result for a fabricated device. Right: theoretical result for a perfect CCR with same size.

$$\frac{d\sigma}{d\Omega_0} = \frac{I_o R^2}{I_i}$$

where I_i is the light intensity incident on the CCR, R is the distance between the CCR and the observing plane, and I_o is the reflected light intensity at the observation plane. For a CCR with side length of 250 µm, DSCS is measured to be 9.3 $\times$ 10^{-4} m^2, while the theoretical result gives 0.044 m^2 [3]. After evaporating 50 nm-thick gold on CCR, the measured DSCS value is increased by 30 times to 0.028m^2, which is quite close to the theoretical result.

Finally, we have realized free-space optical communication over a distance of 180 meters. The CCR is driven by a pseudo-random bit sequence generator at a rate of 400 bps. Figure 8 shows the modulated optical signal detected by a photodiode, as well as the transmitted bit pattern. This bit pattern is received with low error probablity. The amplitude of the modulated signal fluctuates slowly due to air turbulence in the optical path.

CONCLUSION

The modulated CCRs presented here have substantially better performance than any previously presented, due largely to the surprisingly accurate alignment possible by spring-loaded
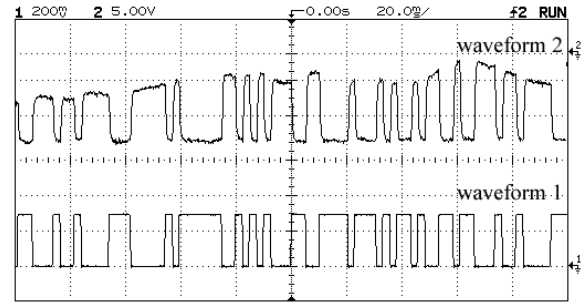

Figure 8: Free-space transmission over 180-meter link. 1: CCR drive signal   2: detected photocurrent, proportional to the intensity reflected from CCR.

assembly of SOI side mirrors. The energy consumption per bit, roughly 40 pJ, is consistent with the power requirements of a millimeter-scale autonomous sensor node [4]. The optical performance of the CCRs is sufficient to allow interrogation from hand-held equipment at ranges of many hundred meters.

ACKNOWLEDGEMENT

REFERENCES

[1] V. S. Hsu, J. M. Kahn, K. S. J. Pister, "MEMS Corner Cube Retroreflectors for Free-space Optical Communications", Masters Thesis, EECS Department, U.C. Berkeley, October 1999.

[2] P. B. Chu, N. R. Lo, E. C. Berg, and K. S. J. Pister, "Optical communication using micro corner cube reflectors", *Proc. of IEEE Micro Electro Mechanical Systems Workshop*, pp. 350-355, Nagoya, Japan, 1997.

[3] X. Zhu, V. S. Hsu and J. M. Kahn, "Optical Modeling of MEMS Corner Cube Retroreflectors with Misalignment and Non-flatness", submitted to *IEEE Journal on Selected Topics in Quantum Electronics*, July 2000.

[4] L. Doherty, B. A. Warneke, B. E. Boser, K. S. J. Pister, "Energy and Performance Considerations for Smart Dust", *Intl. J. Parallel and Distributed Systems*, V4, N3, pp 121-133, 2001